

Increasing the Capacity of Magnetic Induction Communications in RF-Challenged Environments

Zhi Sun, *Member, IEEE*, Ian F. Akyildiz, *Fellow, IEEE*, Steven Kisseleff, *Student Member, IEEE*,
and Wolfgang Gerstaecker, *Senior Member, IEEE*

Abstract—Magnetic Induction (MI) techniques enable efficient wireless communications in dense media with high material absorptions, such as underground soil medium and oil reservoirs. A wide range of novel and important applications in such RF-challenged environments can be realized based on the MI communication mechanism. Despite the potential advantages, the major bottleneck of the MI communication is the limited channel capacity due to the low MI bandwidth. In this paper, the *Spread Resonance (SR) strategy* is developed for the MI communication in RF-challenged environments which greatly increases the MI channel capacity. Specifically, instead of using the same resonant frequency for all the MI coils, the spread resonance strategy allocates different resonant frequencies for different MI relay and transceiver coils. An optimization solution for the resonant frequency allocation is formulated to maximize the MI channel capacity which captures multiple unique MI effects, including the parasitic capacitor in each MI coil, the Eddy currents in various transmission media with limited conductivities, and the random direction of each coil. Numerical evaluations are provided to validate the significant channel capacity improvements by the proposed SR strategy for MI communication systems.

Index Terms—Magnetic induction communications, channel capacity, RF-challenged environments.

I. INTRODUCTION

IN the RF (Radio Frequency)-challenged environments, including the underground soil medium, oil reservoirs, and mines and tunnels, it is extremely difficult to establish reliable and efficient wireless communication [1], [2]. However, many novel and important applications in those RF-challenged environments are recently envisioned to enhance the security or the productivity of our modern society, such as underground oil gas extraction, mine disaster prevention and rescue, concealed border patrol and intruder detection, intelligent agriculturing, underground pipeline tank monitoring, earthquake and landslide forecast, among others [1], [2], [3], [4]. All the above applications require the realization of wireless communication in the RF-challenged environments, which create significant challenges compared to classical electromagnetic (EM) waves

[1]. Specifically, there are two major problems, namely, extremely short communication ranges and highly unreliable channel conditions [1], [5], [6].

Recent developments of the magnetic induction (MI) techniques [7], [8], [9] have great potential to solve the above problems and enable efficient wireless communication in RF-challenged environments. Instead of using propagation waves, the MI-based communication utilizes the near field of a coil. As a result, the MI coils working at HF or lower frequency bands can realize much more reliable channel in the dense medium such as soil and oil. However, the MI-based communication in their original form still suffer from the limited communication range problem due to the high attenuation rate of the magnetic field in the near region.

To enlarge the communication range of the original MI techniques, the MI waveguide technique [10], [11], [12], [13], [14], [15], [16] can be utilized. The MI waveguide consists of multiple resonant relay coils that are deployed in between two nodes. The MI waveguide structure is first proposed in [10], [11], [12], [16], where the relay coils are closely placed so that strong coupling between adjacent coils is formed. In [5], [6], we employed the MI waveguide technique for wireless communication where the relay coils are expected to be placed as sparsely as possible. In this case, the coupling between adjacent relay coils is very weak. The wireless communication between two transceivers is accomplished by the consecutive weak magnetic induction between adjacent MI relay coils, as shown in Fig. 1. By this way, the communication range is greatly enlarged compared to the EM wave-based and the original MI techniques. For example, in the soil medium, the range of the Mica2 sensor is less than 4 m [1]; with similar device size and power, the original MI technique has a communication range around 10 m [5], while the MI waveguide can reach a range of more than 100 m [5]. Moreover, the relay coils in the MI waveguide do not consume extra energy since the magnetic inductions are passively relayed. Those low cost coils are easy to deploy and do not need continuous maintenance. In addition, the lifetime of the wireless system can be greatly prolonged since the MI-based devices can be recharged wirelessly using the inductive charging technique [17], [24]. This property is favorable in RF-challenged environments since it is very difficult to exchange device batteries.

Despite the above advantages, the original MI waveguide-based communication technique has an inherent bottleneck, i.e., the limited channel capacity. Typically, the relative coupling strength (ratio of the mutual induction to the self induc-

Manuscript received August 16, 2012; revised January 18 and April 17, 2013. The editor coordinating the review of this paper and approving it for publication was D. I. Kim.

Z. Sun is with the Department of Electrical Engineering, University at Buffalo, the State University of New York, Buffalo, NY 14260, United States (e-mail: zhisun@buffalo.edu).

I. F. Akyildiz is with the School of Electrical and Computer Engineering, Georgia Institute of Technology, Atlanta, GA 30332, United States (e-mail: ian@ece.gatech.edu).

S. Kisseleff and W. Gerstaecker are with the Institute for Mobile Communications, University of Erlangen-Nurnberg, Erlangen, Germany (e-mail: kisseleff@LNT.de; gerstaecker@nt.e-technik.uni-erlangen.de).

Digital Object Identifier 10.1109/TCOMM.2013.071813.120600

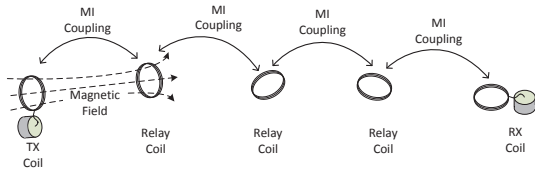


Fig. 1. The MI communication using a MI waveguide.

tion) between adjacent coils in MI waveguide is in the order of 10^{-4} or even smaller. Accordingly, the channel bandwidth of the MI waveguide is very limited [5]. If the transmission distance is increased to a certain threshold, the MI channel bandwidth can be very low [20]. This limited bandwidth corresponds to the very low channel capacity. Therefore, although the MI waveguide-based communication can cover a large range in the RF-challenged environments, the achievable data rate is not satisfactory. In many envisioned applications, such as the border patrol and the mine disaster rescue, a significant volume of data needs to be timely transmitted on the MI channels. Therefore, it is of a great importance to increase the channel capacity in current MI waveguide-based communication systems. The strategy to increase the bandwidth of the strongly coupled MI waveguide has been investigated in [21]. However, to date, the solution to increase channel capacity of the loosely coupled MI waveguide for wireless communication is still not clear.

In this paper, we propose the *Spread Resonance (SR) strategy* for the MI waveguide-based communication system in RF-challenged environments, which can dramatically increase the channel capacity of such systems. In particular, different from the existing MI waveguide where all MI coils use the same resonant frequency, the spread resonance strategy allocates unique and optimal resonant frequencies for different MI relay and transceiver coils. The spread resonance frequencies can effectively enlarge the MI channel bandwidth while the optimal central operating frequency minimizes the path loss. Therefore, the MI channel capacity is greatly increased by the SR strategy. We formulate and solve an optimization problem for the resonant frequency allocation to maximize the MI channel capacity, which captures multiple unique MI effects, including the parasitic capacitance in each MI coil, the Eddy currents in various transmission media with limited conductivities, the background noise as well as the noise generated by the MI waveguide itself, and the random direction of each coil. Finally, comprehensive numerical evaluations are conducted to further validate the channel capacity improvements by the proposed SR strategy for the MI communication systems.

The remainder of the paper is organized as follows. In Section II, the related studies are introduced. In Section III, the SR strategy is developed in detail and the optimal solution is formulated to allocate the resonant frequencies in the SR strategy. Then, in Section IV, numerical studies are performed. Finally, the paper is concluded in Section V.

II. RELATED WORK

Due to the unique advantages of the MI techniques in the RF-impenetrable media, the MI communication systems have been developed in many different scenarios. In [7], an MI

communication system is developed for the naval mine warfare (MIW) operations to provide a reliable wireless command, control and navigation channel. In [8], the MI communication system is used as an alternative to the Bluetooth. The high path loss of MI is utilized to create a personal communication bubble area with minimum interferences. In [9], the MI is used for underground soil medium where it is proven that the MI transmission is not affected by soil properties and requires less power and lower operating frequencies than the EM waves. In [22], the MI technique is implemented in an intra-body network, where the information is transmitted from and to some implanted miniature devices at multiple sites within the human body. In [23], the MI technique is developed to locate and track the underground animals. Through a two-month field experiment, the MI localization system is proven to successfully track wild European badgers within their burrows. In [17], [24], the MI technique is utilized to transfer wireless energy for a relatively long distance. Moreover, the effects of parasitic capacitance of the MI energy transfer system is discussed in [24]. The channel capacity of the above MI communication system that uses a single pair of coils has been investigated in [18], [19]. All the above MI systems use single pairs of MI coils that require either high transmission power or large coil size to reach reasonable transmission ranges.

To enlarge the transmission range, the MI waveguide structure is utilized. The MI waveguide is first proposed in [10] and intensively investigated in [11], [12], [13], [16]. The theoretical results are also validated by the field experiments in [14], [15]. In [25], the impact of the Johnson on the MI waveguide is investigated. In [26], a resonant transducer is developed to reduce the reflection on the terminals of the strongly coupled MI waveguide. Similarly, in [21], a thin-film formed MI waveguide is developed to achieve the low propagation loss and high bandwidth. All the above MI waveguide with strongly coupled relay coils is designed to realize artificial delay filters, dielectric mirrors, distributed Bragg reflectors, among others. However, the above MI waveguide investigations do not cover the applications of wireless communications.

In [6], [5], we introduce the loosely coupled MI waveguide structure in the field of wireless communications, which can greatly enlarge the communication range in many RF-challenged environments without increasing the MI coil size and transmission power. In [27], the channel model of the MI waveguide communication under practical capacitance constraints is derived. The noise models for the MI waveguide communication system are investigated. Besides the point-to-point communication, the MI channel capacity is clearly shown to be extremely low, especially in the far region of the transmitter. Although the MI waveguide-based communication system achieves good transmission range in RF-challenged environments, the above studies focus on minimizing the path loss, while the bandwidth and the channel capacity are not considered at all. Hence, the channel capacity of MI waveguide can be even smaller than that of the original MI system.

In this paper, we propose the SR strategy to enlarge the bandwidth while keeping the path loss on an acceptable level. As a result, the MI channel capacity significantly increases.

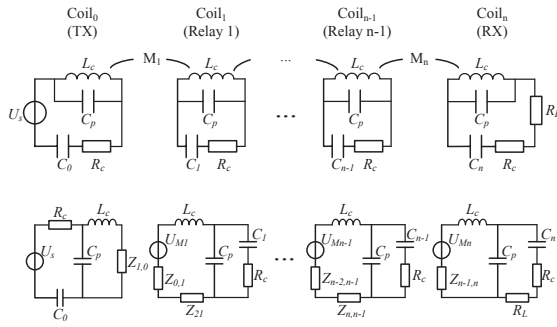


Fig. 2. The high frequency MI waveguide model and the equivalent circuit.

It should be noted that the methods of using multiple resonance frequencies can also be found in other MI systems. However, the objective of the multiple resonance frequencies is different in this paper. For example, in [29], [30], two resonant frequencies are involved in a single MI transceiver: one is for the communications while the other is for the energy transfer. In this paper, we assign spread resonant frequencies to different relay coils, which aims to broaden the MI bandwidth. Moreover, the optimal position of each spread resonant frequency is theoretically determined in this paper.

III. SPREAD RESONANCE STRATEGY

In SR strategy, the resonant frequency of each MI coil is deviated from the original central operating frequency in a controlled manner. The gain of this method is that the MI channel bandwidth can be significantly enlarged if the deviation is properly chosen. However, the drawback of the spread resonant frequency is that the path loss of the MI waveguide system may increase as the resonant frequencies are spread. It is challenging to jointly determine the optimal resonant frequency deviation and the optimal central operating frequency: First, since each MI coil has a unique resonant frequency, it becomes very complicated to calculate the path loss and the bandwidth of the MI waveguide. Consequently, a complicated and non-linear optimization problem is formulated and needs to be solved. Second, since the central operating frequency is expected to be as high as possible to enhance the mutual induction, the impact of the parasitic capacitance [32], [33] of the MI coils cannot be ignored any more. Third, similarly, due to the high central operating frequency, the skin depth effects in the transmission medium caused by the eddy currents [35], [36] need to be modeled for the MI waveguide system, especially in the medium with a not negligible conductivity. In this section, we first formulate the problems of the optimal resonant frequency allocation and central operating frequency selection in the SR strategy. Then, we specifically investigate the influence of the parasitic capacitance and skin depth, respectively. Later we develop the analytical solution of the optimization problem.

A. Problem Formulation

We consider the wireless communications between two transceivers in the RF-challenged environments, especially dense media such as soil, rock, and crude oil. The MI waveguide system consists of $n + 1$ MI coils $\{Coil_0, Coil_1, \dots, Coil_n\}$,

where $Coil_0$ is the transmitter, $Coil_n$ is the receiver, and the rest are relay coils, as shown in Fig. 1. The number of MI coils n is set to be an even number for simplicity. The central operating frequency is denoted as f_0 . The permittivity and the conductivity of the transmission medium are ϵ_m and σ_m , respectively. According to our previous analysis [5], if the transmission medium does not contain magnetites, the permeability of the medium is the same as that of the air, which is μ_0 . It should be noted that in the transmission medium with magnetites, the permeability is higher and the MI performance can be enhanced. However, this situation is out of the scope of this paper since most transmission media in the nature do not contain magnetite material.

Since we only consider the point-to-point communication, there is no interference from other pairs of transceivers. Then, we start from the classic channel capacity formula [31]:

$$C = B \cdot \log_2 \left(1 + \frac{P_t \cdot L_p}{N} \right); \quad (1)$$

where B is the channel bandwidth; P_t is the transmission power; L_p is the path loss; and $N = N_{ambient}$ is the ambient noise power. The average ambient noise power is around -105 dBm, which is measured in underground soil medium [34]. According to our analysis in [5], the path loss L_p is a function of the signal frequency f , i.e. $L_p(f)$. Then based on (1), the channel capacity of the MI waveguide can be calculated as

$$C_{MI} = \int_{f_0 - B/2}^{f_0 + B/2} \log_2 \left(1 + \frac{P_t \cdot L_p(f)}{N_{ambient}} \right) \cdot df; \quad (2)$$

where the transmission power P_t and the ambient noise level $N_{ambient}$ are constants and are determined; while the channel bandwidth B and the path loss $L_p(f)$ need to be designed to maximize the MI channel capacity.

Different from the traditional EM wave-based wireless channel, the MI bandwidth B is not a constant but vary as the configurations of the MI waveguide system change. In addition, the MI waveguide path loss $L_p(f)$ is no longer a simple exponential function due to the consecutive magnetic induction. Moreover, different from the existing analysis [5], [20] on the MI waveguide communication systems, the SR strategy assigns different resonant frequencies to different MI coils and needs to consider the influence of the parasitic capacitance and the skin depth, which create even more challenges in calculating $L_p(f)$, B , and C_{MI} .

Without loss of generality, we denote the resonant frequencies for MI coil $\{Coil_0, Coil_1, \dots, Coil_n\}$ as $f_0 - \frac{n}{2} \cdot \Delta f$, $f_0 - (\frac{n}{2} - 1) \cdot \Delta f$, ..., f_0 , ..., $f_0 + \frac{n}{2} \cdot \Delta f$, where Δf is the frequency interval between two adjacent coils. Δf defines the intensity of how widely the resonant frequency is spread. Then the optimal resonant frequency allocation and central operating frequency selection in SR strategy can be formulated as

- Given* : Transmission distance d ,
Medium permittivity ϵ , Medium conductivity σ ,
Number of MI coils, Coil parameters;
Find : Central operating frequency f_0 ,
Intensity of resonant frequency spread Δf ;
s.t. : MI channel capacity $C_{MI}(f)$ is maximized. (3)

To solve above optimization problem, the MI channel capacity $C_{MI}(f)$ needs to be analytically expressed first. In the following part of this section, we first calculate bandwidth and path loss of the MI waveguide under the SR strategy, where the effects of parasitic capacitance, spread resonant frequencies, and skin depth are accurately modeled. Then, the analytical solution of the optimization problem given in (3) is developed.

B. Modeling the Influence of Parasitic Capacitances and the Spread Resonant Frequencies

In high frequency circuits, the parasitic capacitances are formed due to the distributed electrical coupling between any two conducting objects of the circuit [32]. In MI-waveguides, the MI coils are made of wire loops without the magnetic core and the outer shell. Hence, the coupling between the core and the shell can be ignored. In addition, each MI coil has only one layer of winding. Hence, the layer-to-layer capacitance between two neighboring layers does not exist. Moreover, since the different coils are far enough from each other, the coupling between different coils can be ignored. Therefore, the parasitic capacitances in MI waveguides are formed only due to the coupling between two turns in the winding. In transformer design, the overall effect of parasitic capacitances can be modeled as a lumped capacitor. Since the MI waveguide can be modeled as a multi-stage transformer, the lumped capacitor model is also applicable. Hence, we provide a high frequency transformer model for the MI waveguide system under the SR strategy in the first row in Fig. 2.

In the model, C_p is the lumped capacitor model of the parasitic capacitance in the MI waveguide; M_i ($i = 1, \dots, n$) is the mutual induction between the i^{th} coil and the $(i-1)^{\text{th}}$ coil; U_s is the voltage of the transmitters battery; L_c is the coil self induction; R_c is the wire resistances of the coil; $\{C_i, i = 0, 1, \dots, n\}$ are the capacitors loaded in the i^{th} coil; R_L is the matched load of the receiver that maximizes the received power at the central operating frequency f_0 . It should be noted that with the signal frequency deviation from the central frequency, there will be reflected power from the MI receiver that causes additional path loss. All MI coils have the same configurations expect the loaded capacitor $\{C_i, i = 0, 1, \dots, n\}$, which is used to achieve the resonant status on the resonant frequency. Since different coils are allocated different resonant frequencies in SR strategy, the loaded capacitances C_i are also different. Other than the loaded capacitances, all the coils have the same parameters, including the wire resistance R_c , coil radius a , and number of turns N_t . The equivalent circuits of the high frequency multi-stage transformer is shown in the second row in Fig. 2, where

$$U_{M_i} = -j\omega M_i \cdot \frac{U_{M_{i-1}}}{Z_{i-2,i-1} + j\omega L_c + \frac{\frac{1}{j\omega C_p} \cdot (\frac{1}{j\omega C_{i-1}} + R_c)}{\frac{1}{j\omega C_p} + \frac{1}{j\omega C_{i-1}} + R_c}}, \quad (i = 2, 3, \dots, n);$$

$$U_{M_1} = -j\omega M_1 \cdot \frac{U_s}{\frac{1}{j\omega C_0} + R_c + \frac{\frac{1}{j\omega C_p} \cdot j\omega L_c}{\frac{1}{j\omega C_p} + j\omega L_c}} \cdot \frac{1}{\frac{1}{j\omega C_p} + j\omega L_c};$$

$$Z_{i,i-1} = \frac{\omega^2 M_i^2}{j\omega L_c + Z_{i+1,i} + \frac{\frac{1}{j\omega C_p} \cdot (\frac{1}{j\omega C_i} + R_c)}{\frac{1}{j\omega C_p} + \frac{1}{j\omega C_i} + R_c}}, \quad (i = 1, 2, \dots, n-1);$$

$$Z_{n,n-1} = \frac{\omega^2 M_n^2}{j\omega L_c + \frac{\frac{1}{j\omega C_p} \cdot (\frac{1}{j\omega C_n} + R_c + Z_L)}{\frac{1}{j\omega C_p} + \frac{1}{j\omega C_n} + R_c + Z_L}};$$

$$Z_{i-1,i} = \frac{\omega^2 M_i^2}{j\omega L_c + Z_{i-2,i-1} + \frac{\frac{1}{j\omega C_p} \cdot (\frac{1}{j\omega C_0} + R_c)}{\frac{1}{j\omega C_p} + \frac{1}{j\omega C_0} + R_c}}, \quad (i = 2, 3, \dots, n);$$

$$Z_{0,1} = \frac{\omega^2 M_1^2}{j\omega L_c + \frac{\frac{1}{j\omega C_p} \cdot (\frac{1}{j\omega C_0} + R_c)}{\frac{1}{j\omega C_p} + Z_{i+1,i} + \frac{1}{j\omega C_0} + R_c}}. \quad (4)$$

In (4), f is the signal frequency and $\omega = 2\pi f$ is the corresponding angle frequency; the coil self induction $L_c = \frac{1}{2}\mu\pi N_t^2 a$; the coil wire resistances $R_c = N_t \cdot 2\pi a \cdot R_0$ where R_0 is the unit length resistance of the wire determined by the material and thickness; $Z_{i(i-1)}$ is the influence of the i^{th} coil on the $(i-1)^{\text{th}}$ coil and vice versa; U_{M_i} is the induced RMS (root mean square) voltage on the i^{th} coil; U_s is the RMS voltage of the signal at the transmitter coil. The mutual inductions M_i is substantially influenced by the skin depth effect, which will be discussed in the next subsection.

We utilize a method proposed in [33] to determine the lumped capacitor model C_p for the parasitic capacitance in the MI waveguide system. We assume that the coating material of the wire on the coil has a relative permittivity ϵ_c ; the diameter of the bare wire is D_b ; and the diameter of the coated wire is D_c . Then, the value of the parasitic capacitance C_p can be calculated by the following formula:

$$C_p = \frac{1}{N_t - 1} \cdot \epsilon_0 \cdot 2\pi a \cdot \left[\frac{\epsilon_c' \cdot \arccos(1 - \frac{\ln \frac{D_c}{D_b}}{\epsilon_c'})}{\ln \frac{D_c}{D_b}} + \cot \left(0.5 \arccos(1 - \frac{\ln \frac{D_c}{D_b}}{\epsilon_c'}) \right) - \cot \left(\frac{\pi}{12} \right) \right]; \quad (5)$$

where ϵ_0 is the permittivity of the vacuum permittivity; and $\epsilon_c' = \frac{\epsilon_c}{\epsilon_0}$ is the relative permittivity of the wire coating material. According to (5), we can control the parasitic capacitance at an acceptable value by: 1) increasing the number of turns of the coil; 2) using thicker wire coating; and 3) using coating material with lower permittivity.

By utilizing the multi-stage high frequency transformer model and its equivalent circuit, the path loss and the bandwidth of the MI waveguide communication system can be calculated. Before calculating the MI channel capacity, we need to solve the remaining question, i.e. modeling the skin depth effects on the mutual induction M_i .

C. Modeling the Influence of Skin Depth

The skin depth describes how the time-varying EM field is distributed within a conductive material, i.e. how deep the EM field can exist beneath the surface of the conductor. In RF-challenged environments, although the transmission medium generally consists of non-conductive materials, it can have a certain level of conductivity under certain circumstances, such as in wet soil, oil reservoirs, and copper mines. If the operating frequency is low, the skin depth is very large and the EM field can be considered to exist anywhere in the medium. Hence, the skin depth can be ignored. However, in SR strategy, the operating frequency is supposed to be as high as possible.

Then, the skin depth become much smaller. Consequently, the EM field has enough strength only within a shorter range around the MI coil. Beyond this range, the EM field may become extremely weak.

The small skin depth can significantly weaken the mutual induction between adjacent MI coils in a MI waveguide communication system, which induces the additional loss of the magnetic field. According to [5], the MI coil is modeled as a magnetic dipole since the intervals between adjacent coils are much larger than the coil size. Hence, the mutual induction can be deduced by the magnetic potential A of the magnetic dipole. The expression of A in non-conductive medium is provided in [5]. However, in SR strategy, A will have an additional attenuation factor G due to the skin depth effect. The additional attenuation factor G is a function of the distance between the two MI coils r and the skin depth δ in the medium. $G(r, \delta)$ can be calculated according to the model provided in [35], where

$$G(r, \delta) = \left| \int_0^{\infty} \frac{x^3}{x + [x^2 + j(\frac{\sqrt{2}r}{\delta})^2]^{\frac{1}{2}}} \cdot \exp[-x^2 - j(\frac{\sqrt{2}r}{\delta})^2]^{\frac{1}{2}} \cdot dx \right|. \quad (6)$$

The skin depth δ is a function of the operating frequency, the medium permeability μ , the medium permittivity ϵ , and the medium conductivity σ , which can be calculated by [36]:

$$\delta = \frac{1}{\omega \sqrt{\frac{\mu\epsilon}{2} \left(\sqrt{1 + \frac{\sigma^2}{\omega^2\epsilon^2}} - 1 \right)}}. \quad (7)$$

The skin depth effect can be accurately characterized by the additional attenuation factor $G(r, \delta)$ in (6). However, (6) contains integral computations that is not favorable in most optimization problems. Hence, we approximate (6) by a simpler function of the ratio of coil interval r and skin depth δ . By analyzing the numerical results of (6), we can approximately match $G(r, \delta)$ as an exponential function of $\frac{r}{\delta}$ as follows:

$$G(r, \delta) \approx 1.004 \cdot \exp\left(-0.1883 \cdot \left(\frac{r}{\delta}\right)^{1.671}\right). \quad (8)$$

where the data fitting is conducted under the condition that the relative skin depth $\frac{r}{\delta}$ is in the range from 0 to 10. It should be noted that $G(r, \delta)$ is almost 0 when $\frac{r}{\delta} = 10$. Since $G(r, \delta)$ is monotonically decreasing and non-negative, the approximation done in (8) is applicable for all values of $\frac{r}{\delta}$ from 0 to infinity.

Then, the mutual induction of the i^{th} coil and the $(i-1)^{\text{th}}$ coil can be calculated by:

$$M_i \approx \mu\pi N_t^2 \frac{a^4}{4r^3} G(r_i, \delta) \cdot (2 \sin \theta_i^j \sin \theta_r^j + \cos \theta_i^j \cos \theta_r^j), \quad (9)$$

where r_i is the distance between the i^{th} coil and the $(i-1)^{\text{th}}$ coil; θ_i^j and θ_r^j are the angles between the coil radial directions and the line connecting the two coils.

D. Optimization Solution

By substituting (5) and (9) into (4), the equivalent circuit model of the MI waveguide system under the SR strategy is completed. Given the circuit parameters, the received power P_r at the receiver coil can be calculated. By investigating

the P_r as functions of the transmission distance and the operating frequency, the path loss and the bandwidth of the MI waveguide communication system can be derived.

To obtain the lowest path loss, the loaded capacitor should be as small as possible to achieve high operating frequency. However, according to the equivalent circuit model given in (4), if the loaded capacitor is smaller than the parasitic capacitance, it cannot effectively control the resonant frequency. Instead, the parasitic capacitance would determine the resonant frequency. Therefore, to keep the resonant frequency under control, the bottom line is to that the loaded capacitor should be larger than the parasitic capacitance. In this paper, our objective is to maximize the MI channel capacity and we want the smallest path loss and the largest bandwidth. Therefore, we let the loaded capacitor have a value on par with the parasitic capacitance. As a result, the path loss of the MI waveguide can be minimized while we can still tune the value of the loaded capacitor to assign optimal resonant frequency to each MI coils. Based on the above discussion, we can calculate the received power P_r with matched load as follows:

$$P_r \approx \frac{1}{4} \cdot \left| \frac{2 \cdot Z_{n-1,n} + R_c}{(j\omega L_c + \frac{1}{2} \frac{1}{j\omega C_n} + 2 \cdot Z_{n-1,n} + R_c)^2} \right| \cdot \left| U_s \cdot \frac{M_1}{L_c} \cdot \frac{-j\omega M_2}{Z_{0,1} + j\omega L_c + \frac{1}{2}(\frac{1}{j\omega C_1} + R_c)} \cdot \dots \cdot \frac{-j\omega M_n}{Z_{n-2,n-1} + j\omega L_c + \frac{1}{2}(\frac{1}{j\omega C_{n-1}} + R_c)} \right|^2, \quad (10)$$

In (10), $Z_{i,i-1}$ and $Z_{i-1,i}$ are the coupled impedance that the adjacent coils put on each other. $Z_{i,i-1}$ and $Z_{i-1,i}$ have significant effects only if the coils are closely placed (i.e. the interval r_i between adjacent coils is small enough). However, one of the design objectives is to use as few relay coils as possible to reduce the deployment and maintenance cost. According to the numerical calculations using (4), $Z_{i,i-1}$ and $Z_{i-1,i}$ can be safely neglected if the ratio of the coil interval and the coil size (radius) $\frac{r_i}{a}$ is larger than 10, which is applicable in most envisioned applications. Hence, by using (10) while ignoring the coupled impedances, the path loss of the MI waveguide system under the SR strategy can be calculated:

$$L_p(\omega) \approx \frac{1}{4} \cdot \left| \frac{R_c^2}{(j\omega L_c + \frac{1}{2} \frac{1}{j\omega C_n} + R_c)^2} \right| \cdot \left| \frac{M_1}{L_c} \cdot \frac{-j\omega M_2}{j\omega L_c + \frac{1}{2}(\frac{1}{j\omega C_1} + R_c)} \cdot \dots \cdot \frac{-j\omega M_n}{j\omega L_c + \frac{1}{2}(\frac{1}{j\omega C_{n-1}} + R_c)} \right|^2. \quad (11)$$

It should be noted that the transmission power P_t used for calculating the MI path loss is the maximum power at the transmitter, i.e., $P_t^{\max} = \frac{U_s^2}{R_c}$. The reason is that the actual transmission power of the MI communication systems decreases as the transmission distance increases. Less power can be emitted as the MI coils are placed further to each other. Hence, using the actual transmission power results in an unrealistically small value for the path loss, which cannot characterize the MI channel. By using the maximum transmission power, the path loss cannot be underestimated.

In SR strategy, the bandwidth of the MI waveguide is determined by how widely the resonant frequency is spread:

$$B = n \cdot \Delta f. \quad (12)$$

Fluctuations may exist inside the bandwidth since the path loss reaches its local minima at each resonant frequency of the MI coils, which can be eliminated by channel equalizations.

Then, by substituting (11) and (12) into (2), the MI channel capacity can be calculated. To avoid the integral in the optimization, we select a single frequency, i.e. $f = f_0 - \frac{n-1}{2} \cdot \Delta f$, in calculating the path loss $L_p(2\pi f)$ in (13). At such frequency, the MI waveguide system achieves maximum in-band path loss due to the following two reasons: 1) MI waveguide path loss achieves its local maxima at the frequency in the middle of two adjacent resonant frequencies; and 2) the overall path loss increases as the signal frequency deviates from the central operating frequency. Therefore, all the path loss inside the bandwidth is guaranteed to be lower than the path loss at $f_0 - \frac{n-1}{2} \cdot \Delta f$. Due to this reason, the actual system channel capacity can be slightly higher than theoretical one derived in this paper. Moreover, to guarantee correct demodulation, the signal to noise ratio is expected to be sufficiently large. Hence, the constant 1 inside the logarithm function can be neglected. Then, the MI channel capacity in (1) can be deduced as

$$\begin{aligned} C_{MI} &\approx n \cdot \Delta f \cdot \log_2 \left\{ \frac{P_t \cdot L_p \left[2\pi \left(f_0 - \frac{n-1}{2} \cdot \Delta f \right) \right]}{N_{ambient}} \right\} \\ &= n \cdot \Delta f \cdot \left[\log_2 \left(\frac{P_t}{N_{ambient}} \cdot \frac{R_c^2}{4\omega L_c} \right) + 2 \sum_{i=1}^n \log_2 |\omega M_i| \right. \\ &\quad \left. - 2 \sum_{i=1}^n \log_2 \left| j\omega L_c + \frac{1}{2j\omega C_i} + \frac{R_c}{2} \right| \right]; \end{aligned} \quad (13)$$

where $\omega = 2\pi \left(f_0 - \frac{n-1}{2} \cdot \Delta f \right)$; C_i is set to the value to achieve the resonant status at the frequency $f_0 + (i - \frac{n}{2}) \cdot \Delta f$, i.e.

$$\frac{1}{j4\pi [f_0 + (i - \frac{n}{2}) \cdot \Delta f] \cdot C_i} + j2\pi [f_0 + (i - \frac{n}{2}) \cdot \Delta f] \cdot L_c = 0; \quad (14)$$

Then the MI channel capacity can be further developed as:

$$\begin{aligned} C_{MI} &= n \cdot \Delta f \cdot \left[\log_2 \left(\frac{P_t}{N_{ambient}} \cdot \frac{R_c^2}{4\omega L_c} \right) + 2 \sum_{i=1}^n \log_2 |\omega M_i| \right. \\ &\quad \left. - 2 \sum_{i=1}^n \log_2 \left| j2\pi \cdot \frac{[2f_0 + (i + \frac{1}{2} - n)\Delta f] \cdot (\frac{1}{2} - i)\Delta f}{f_0 - \frac{n-1}{2} \cdot \Delta f} \cdot L_c + \frac{R_c}{2} \right| \right]; \end{aligned} \quad (15)$$

Since the resonant frequency deviation $i \cdot \Delta f$, ($i = 1, 2, \dots, n$) is much smaller than central operating frequency f_0 , the channel capacity formula can be further developed as

$$\begin{aligned} C_{MI} &\approx n \cdot \Delta f \cdot \left[\log_2 \left(\frac{P_t}{N_{ambient}} \cdot \frac{R_c^2}{4\omega L_c} \right) + 2 \sum_{i=1}^n \log_2 (2\pi f_0 \cdot |M_i|) \right. \\ &\quad \left. - 2 \sum_{i=1}^n \log_2 \left| j2\pi \cdot (1 - 2i)\Delta f \cdot L_c + \frac{R_c}{2} \right| \right]; \end{aligned} \quad (16)$$

As mentioned in Section III-C, the mutual inductions M_i between the MI coils are random variables since the position and the directions of each MI coils may vary in different locations as time elapses. Therefore, the MI channel capacity is also

a random variable. In the optimization problem addressed in this paper, we aim to maximize the ε -outage channel capacity $\text{Outage}_\varepsilon[C_{MI}]$, which is the channel capacity that the MI communication system can achieve with a probability $1 - \varepsilon$.

Since the coils are supposed to be deployed in dense medium like underground soil medium, it is unlikely that the coils can be shifted a distance longer than the dimension of the coil once the coils are deployed. Moreover, the coil interval length is much longer than the coil size in MI communication systems. Therefore, within the deviation limit, the influence of the deviations of the intervals r_i can be neglected. However, the directions of the coils can be highly random in some specific applications, such as the oil reservoir monitoring. Assuming each MI coil has an independent and identically distributed (i.i.d) direction, the MI channel capacity can be approximately viewed as a Gaussian random variable, which can be proven as follows. According to (16), only the second term in the MI channel capacity formula is a random variable. This term is the sum of the logarithm functions of the mutual induction of each MI coil. Since the value of the mutual induction of each coil is i.i.d and the MI waveguide usually consists of many relay coils, the term $\sum_{i=1}^n \log [2\pi f_0 \cdot |M_i|]$ approximately follows the normal distribution according to the central limit theorem [37]. Since the other two terms in (16) are not random variables, the total MI channel capacity also follows the normal distribution. The mean value of the MI channel capacity can be approximately expressed as

$$\begin{aligned} E[C_{MI}] &= n \cdot \Delta f \cdot \left[\log_2 \left(\frac{P_t}{N_{ambient}} \cdot \frac{R_c^2}{4\omega L_c} \right) + 2n \cdot \log_2 (2\pi f_0 \cdot |M^0(f_0)|) \right. \\ &\quad \left. - 2 \sum_{i=1}^n \log_2 \left| j2\pi \cdot (1 - 2i)\Delta f \cdot L_c + \frac{R_c}{2} \right| \right]; \end{aligned} \quad (17)$$

where $M^0(f_0)$ is the initial direction or the designed direction of each coil. There two types of the designed directions of MI coils: the axial alignment and the planar alignment. In the axial alignment, $\theta_r^i = 0$ and $\theta_t^i = 0$; while in the planar alignment, $\theta_r^i = \frac{\pi}{2}$ and $\theta_t^i = \frac{\pi}{2}$. It should be noted that $M^0(f_0)$ is still a function of the central operating frequency f_0 since the skin depth takes effect at any directions of the coils.

The variance of the MI channel capacity $\text{Var}[C_{MI}]$ cannot be analytically calculated since it depends on the specific applications and environments, which can be dramatically different from case to case. Therefore, in this paper, we set the variance of the MI channel capacity as $q\%$ of the mean capacity, where the value of q defines how severely the coil directions may deviate from the designed value. Then, the ε -outage channel capacity $\text{Outage}_\varepsilon[C_{MI}]$ can be calculated as

$$\text{Outage}_\varepsilon[C_{MI}] = E[C_{MI}] + \text{erf}^{-1}(2\varepsilon - 1) \cdot \sqrt{2\text{Var}[C_{MI}]}. \quad (18)$$

Now the optimization problem given in (3) can be realized:

$$\begin{aligned} \text{Find} &: f_0, \Delta f \\ \text{Maximize} &: \text{Outage}_\varepsilon[C_{MI}] \\ \text{Subject to} &: f_0 + \frac{n}{2} \cdot \Delta f < \frac{1}{2\pi \sqrt{L_c \cdot C_p}} \end{aligned} \quad (19)$$

where C_p is the lumped model of the parasitic capacitance, which is given by (5). The constraints in (19) are due to the

fact that the loaded capacitor should be larger than the parasitic capacitance, as discussed previously.

Although the problem in (19) is a nonlinear programming, it can be solved by the convex optimization methods [38], especially the Lagrange multiplier, due to the following reasons: 1) the ε -outage channel capacity $\text{Outage}_\varepsilon[C_{MI}]$ is a concave function of the central frequency f_0 and the spread intensity Δf ; and 2) the constraint set $f_0 + \frac{n}{2} \cdot \Delta f < \frac{1}{2\pi\sqrt{L_c \cdot C_p}}$ is convex. Hence, the optimal central operating frequency f_0 and the optimal spread intensity Δf in the SR strategy can be derived by solving the convex programming problem defined in (19). Since (19) is already the standard form of a convex programming problem, it would be trivial to show the detailed procedure of classic Lagrange multiplier method to solve the convex programming problem in this paper. In next section, we will discuss the optimization results in details based on the numerical evaluations.

IV. NUMERICAL EVALUATION

In this section, the performance of the SR strategy is evaluated by Matlab numerical results. The effects of the transmission distance, the parasitic capacitance, the skin depth, and the coil direction rotations on the maximum MI channel capacity, the optimal operating frequency, and the intensity of the spread resonant frequency are quantitatively captured. The MI channel capacity optimized by the SR strategy is also compared with the capacity of the original MI waveguide communication system, which validates the dramatic capacity increase of the proposed strategy. We use the 10-dB bandwidth to calculate the channel capacity of the original MI waveguide. It should be noted that the capacity contribution from the signal that has a received power more than 10 dB lower than the power at the central frequency can be neglected.

In the evaluations, except studying the effects of certain parameters, the default values are set as follows: The MI waveguide consists of MI coils with the radius of 0.5 m. The number of turns of each coil is $N = 10$. The coils are deployed every $r = 5$ m. The total number of coils n are determined by the transmission distance d , i.e., $n = \lceil \frac{d}{r} \rceil$. The coils are made of cooper wire with 4 mm diameter and 2 mm thick coating material. The unit resistance of such copper wire is $0.5 \Omega/km$. The relative permittivity of the coating material is 2. The parasitic capacitance of such MI coil can be calculated by (5), which is 51 pF. As discussed in the beginning, the permeability of the transmission medium is the same as that in the air, i.e. $\mu_0 = 4\pi \times 10^{-7}$ H/m. The conductivity of the transmission medium $\sigma = 0.0005$ S/m. The transmission power is set as 10 dBm (10 mW) and the background noise level is -105 dBm. As discussed in the last section, the effect of the random coil direction is characterized by the ratio of the capacity variance and the capacity mean value, which is set to 20 % as the default value in the analysis.

In Fig. 3, the 20%-outage channel capacity is given as a function of the central operating frequency f_0 and the spread intensity of the resonant frequency Δf . As expected, the MI channel capacity is a concave function of f_0 and Δf , which justifies the effectiveness of the Lagrange multiplier optimization method. As shown in Fig. 3, the spread intensity

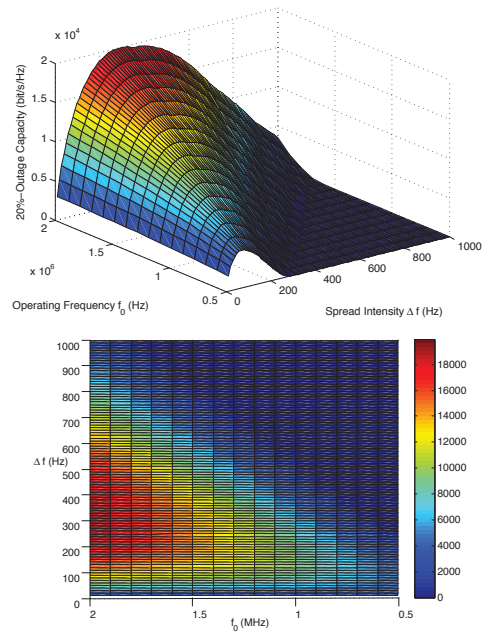
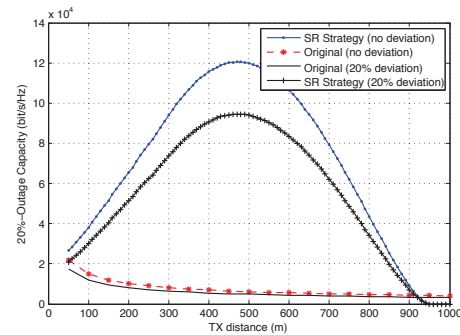
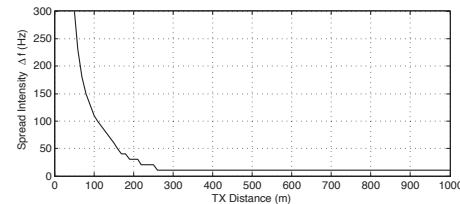


Fig. 3. The 20%-Outage channel capacity as a function of the central operating frequency and the spread intensity of the resonant frequency.



(a) The optimal 20%-outage capacity with/without coil direction deviations as a function of transmission distance.



(b) The optimal spread intensity of the resonant frequency as a function of transmission distance.

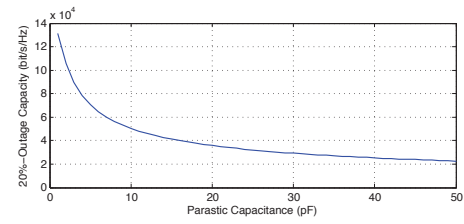
Fig. 4. Effects of transmission distance and random coil directions.

Δf ranges from 0 to 1000 Hz. There is an optimal intensity for each central operating frequency that can maximize the MI channel capacity. The central operating frequency f_0 ranges from 500 KHz to the maximum operating frequency, which is constrained by the parasitic capacitance as shown in (19). The MI channel capacity in Fig. 3 is a monotonically increasing function of f_0 in this range. The reason for the monotonic increase is that the medium conductivity is not very high in Fig. 3. Hence, the skin depth effect is not significant for the coil interval length. As a result, the constraint only comes from the parasitic capacitance in this scenario.

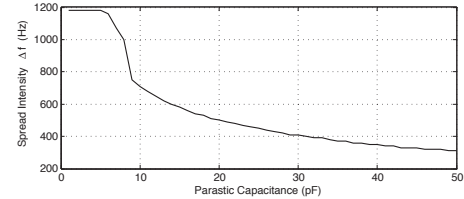
In Fig. 4(a), the 20%-outage channel capacity with and without coil direction deviations is given as a function of transmission distance. The capacity of the original MI waveguide communication with the same parameters is also plotted for comparison. As shown in Fig. 4(a), the SR strategy achieves a MI channel capacity that is much higher than the original MI waveguide system, especially in the far region. The reason for the significant capacity increase can be explained as follows. If the MI coils are deployed close enough to maintain sufficient coupling, the path loss can be controlled in a low level even the transceivers are hundreds of meters apart from each other. However, in the original MI waveguide system, the system bandwidth dramatically decreases as the number of relay coils increases. The SR strategy solves this problem by assigning unique and optimal resonant frequency for each MI coil to tradeoff the low path loss and the high bandwidth, which results in a much higher channel capacity. An interesting phenomenon is that the MI channel capacity under SR strategy increases as the transmission distance increases at first. This is due to the fact that more relay coils are used when the distance increases. More relay coils means that the resonant frequencies are spread more widely. However, after a certain distance, the MI channel capacity starts to decrease. This is due to the reason that the system path loss increases dramatically when the transmission distance is larger than a threshold. Fig. 4(a) also indicates that the random directions of the MI coils significantly affect the MI channel capacity, especially in the SR strategy that highly depends on the mutual induction between adjacent coils. In Fig. 4(b), the optimal spread intensity of the resonant frequency is given as a function of transmission distance. As expected, the optimal spread intensity decreases as the transmission distance increases, which can lower the path loss in the far region. As discussed previously, when the medium conductivity is low, it is always optimal to choose the maximum central operating frequency no matter how large the transmission distance is.

In Fig. 5, the effects of the parasitic capacitance on the SR strategy are investigated. Fig. 5(a) shows the optimal 20%-outage channel capacity as a function of parasitic capacitance; Fig. 5(b) gives the optimal frequency spread intensity as a function of parasitic capacitance; and Fig. 5(c) provides the optimal central operating frequency as a function of parasitic capacitance. As the parasitic capacitance increases, the allowed maximum operating frequency also decreases. Since the medium conductivity is not very high, the optimal operating frequency equals the maximum operating frequency, which decreases as the parasitic capacitance increases. Lower operating frequency causes weaker mutual magnetic coupling and smaller optimal frequency spread intensity. Therefore, the optimal MI channel capacity also dramatically decreases as the parasitic capacitance increases.

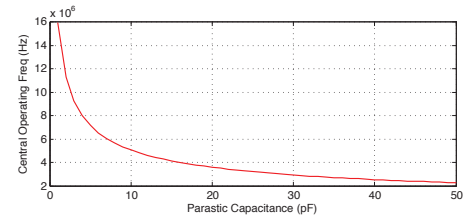
In Fig. 6, the effects of the medium conductivity or the skin depth on the SR strategy is analyzed. Fig. 6(a), Fig. 6(b), and Fig. 6(c) give the optimal 20%-outage channel capacity, the optimal frequency spread intensity, and the optimal central operating frequency as functions of the medium conductivity, respectively. As the medium conductivity increases, the mutual induction between adjacent coils is weakened due to the smaller skin depth. Hence, the optimal frequency spread inten-



(a) The optimal 20%-outage channel capacity as a function of parasitic capacitance.



(b) The optimal spread intensity of the resonant frequency as a function of parasitic capacitance.



(c) The optimal central operating frequency as a function of parasitic capacitance.

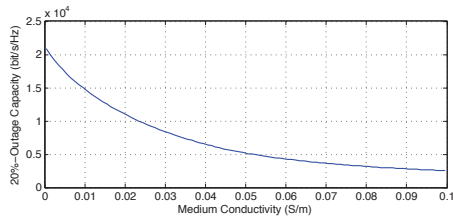
Fig. 5. Effects of parasitic capacitance.

sity decreases accordingly to compensate the weakened mutual induction. The optimal MI channel capacity also decreases as the medium conductivity increases. To achieve the optimal MI channel capacity, the maximum central operating frequency is selected when the medium conductivity is smaller than a threshold, since the higher operating frequency enhances the induced voltage U_{MI} at each MI coil while the skin depth is still not too small. However, when the medium conductivity is larger than the threshold, higher operating frequency causes much smaller skin depth. As a result, the optimal operating frequency is smaller than the maximum operating frequency.

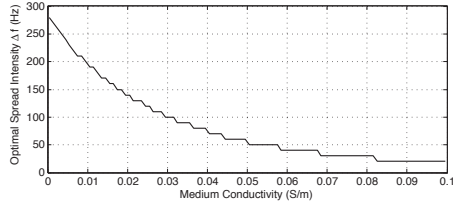
V. CONCLUSION

In this paper, we propose the Spread Resonance (SR) strategy to increase the channel capacity of the MI waveguide communication systems in RF-challenged environments. Unique resonant frequency is optimally allocated for each MI relay coils and transceiver coils. As a result, the received power is not concentrated at the single central operating frequency but is spread among the multiple resonant frequencies. We formulate an optimization problem for the resonant frequency allocation to maximize the MI channel capacity, which can be solved by the Lagrange multiplier method. Multiple unique MI effects are analytically captured in the optimization, including the parasitic capacitor in each MI coil, the skin depth in various transmission media with limited conductivities, and the random direction of each coil.

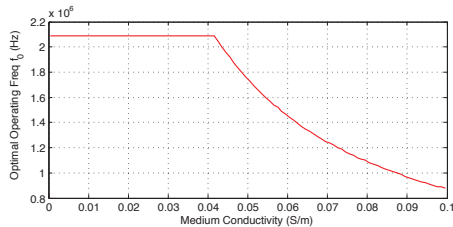
Through the theoretical analysis and numerical evaluations, we find significant channel capacity improvements in the



(a) The optimal 20%-outage channel capacity as a function of medium conductivity.



(b) The optimal spread intensity of the resonant frequency as a function of medium conductivity.



(c) The optimal central operating frequency as a function of medium conductivity.

Fig. 6. Effects of medium conductivity and skin depth.

MI waveguide communication system if the proposed SR strategy is applied. Since the adjacent coil in the MI waveguide communication system is very weakly coupled to minimize the number of relay coils, there exists a tradeoff between larger bandwidth and lower MI path loss. The SR strategy utilizes this tradeoff and find the optimal balance by letting each MI coils working at different pre-designed resonant frequencies. Despite the advantages, the system complexity is significantly increased since each relay coil in a MI waveguide is different from each other now. The system deployment also becomes more difficult due to the non-homogeneous MI waveguide. To solve this problem in the future, more advanced MI waveguide structures other than simple resonant coils need to be investigated. For example, the thin-film MI waveguide [21] provided an improved structure to enhance both the MI bandwidth and received signal strength in the strong mutual coupling applications. It remains an open research issue to find out advanced MI waveguide structure to improve the performance of the MI-based wireless communications where the mutual coupling is very weak.

ACKNOWLEDGMENT

This work was supported by the German Research Foundation (Deutsche Forschungsgemeinschaft, DFG) under Grant No. GE 861/4-1 and the Start-up Grant from the School of Engineering, State University of New York at Buffalo.

REFERENCES

- [1] I. F. Akyildiz, Z. Sun, and M. C. Vuran, "Signal propagation techniques for wireless underground communication networks," *Physical Commun. J.*, vol. 2, no. 3, pp. 167–183, Sep. 2009.
- [2] Z. Sun and I. F. Akyildiz, "Key communication techniques for underground sensor networks," *Foundations and Trends in Networking*, vol. 5, no. 4, pp. 138–283, 2012.
- [3] Z. Sun, *et al.*, "BorderSense: border patrol through advanced wireless sensor networks," *Ad Hoc Networks J.*, vol. 9, no. 3, pp. 468–477, May 2011.
- [4] Z. Sun, *et al.*, "MISE-PIPE: magnetic induction-based wireless sensor networks for underground pipeline monitoring," in *Ad Hoc Networks J.*, vol. 9, no. 3, pp. 218–227, May 2011.
- [5] Z. Sun and I. F. Akyildiz, "Magnetic induction communications for wireless underground sensor networks," *IEEE Trans. Antennas Propag.*, vol. 58, no. 7, pp. 2426–2435, July 2010.
- [6] Z. Sun and I. F. Akyildiz, "Underground wireless communication using magnetic induction," in *Proc. 2009 IEEE ICC*.
- [7] J.J. Sojdecki, P. N. Wrathall, and D. F. Dinn, "Magneto-inductive (MI) communications," in *Proc. 2001 MTS/IEEE Conference and Exhibition*.
- [8] R. Bansal, "Near-field magnetic communication," *IEEE Antennas and Propag. Mag.*, Apr. 2004.
- [9] N. Jack and K. Shenai, "Magnetic induction IC for wireless communication in RF-impenetrable media," in *Proc. 2007 IEEE Workshop on Microelectronics and Electron Devices*.
- [10] E. Shamonina, V. A. Kalinin, K. H. Ringhofer, and L. Solymar, "Magneto-inductive waveguide," *Electron. Lett.*, vol. 38, no. 8, pp. 371–373, Apr. 2002.
- [11] R. R. A. Syms, I. R. Young, and L. Solymar, "Low-loss magneto-inductive waveguides," *J. Physics D: Applied Physics*, vol. 39, pp. 3945–3951, 2006.
- [12] E. Shamonina, V. A. Kalinin, K. H. Ringhofer, and L. Solymar, "Magneto-inductive waves in one, two, and three dimensions," *J. Applied Physics*, vol. 92, no. 10, pp. 6252–6261, 2002.
- [13] R. R. A. Syms, E. Shamonina, and L. Solymar, "Magneto-inductive waveguide devices," in *Proc. IEE Microwaves, Antennas and Propagation*, vol. 153, no. 2, pp. 111–121, 2006.
- [14] M. C. K. Wiltshire, E. Shamonina, I. R. Young, and L. Solymar, "Dispersion characteristics of magneto-inductive waves: comparison between theory and experiment," *Electron. Lett.*, vol. 39, no. 2, pp. 215–217, 2003.
- [15] C. J. Stevens, C. W. T. Chan, K. Stamatis, and D. J. Edwards, "Magnetic metamaterials as 1-D data transfer channels: an application for magneto-inductive waves," *IEEE Trans. Micr. Theory Tech.*, vol. 58, pp. 1248–1256, 2010.
- [16] L. Solymar and E. Shamonina, *Waves in Metamaterials*. Oxford University Press, 2009.
- [17] A. Karalis, J. D. Joannopoulos, and M. Soljacic, "Efficient wireless non-radiative mid-range energy transfer," *Annals of Physics*, vol. 323, no. 1, pp. 34–48, Jan. 2008.
- [18] H. Jiang and Y. Wang, "Capacity performance of an inductively coupled near field communication system," in *Proc. 2008 IEEE International Symposium of Antenna and Propagation Society*.
- [19] J. I. Agbinya and M. Masihpour, "Power equations and capacity performance of magnetic induction communication systems," *Wireless Personal Commun. J.*, vol. 64, no. 4, pp. 831–845, 2012.
- [20] Z. Sun and I. F. Akyildiz, "On capacity of magnetic induction-based wireless underground sensor networks," in *Proc. 2012 IEEE INFOCOM*.
- [21] R. R. A. Syms, L. Solymar, I. R. Young, and T. Floume, "Thin-film magneto-inductive cables," *J. Physics D: Applied Physics*, vol. 43, no. 5, 2010.
- [22] M. Sun, S. A. Hackworth, Z. Tang, G. Gilbert, S. Cardin, and R. J. Scabassi, "How to pass information and deliver energy to a network of implantable devices within the human body," in *Proc. 2007 IEEE Conference on Engineering in Medicine and Biology Society*, pp. 5286–5289.
- [23] A. Markham, N. Trigoni, S. A. Ellwood, and D. W. Macdonald, "Revealing the hidden lives of underground animals using magneto-inductive tracking," in *Proc. 2010 SenSys*.
- [24] C. S. Wang, G. A. Covic, and O. H. Stielau, "Power transfer capability and bifurcation phenomena of loosely coupled inductive power transfer systems," *IEEE Trans. Industrial Electron.*, vol. 51, no. 1, pp. 148–157, 2004.
- [25] R. R. A. Syms and L. Solymar, "Noise in metamaterials," *J. Applied Physics*, vol. 109, no. 12, 2011.

- [26] R. R. A. Syms, L. Solymar, and I. R. Young, "Broadband coupling transducers for magneto-inductive cables," *J. Physics D: Applied Physics*, vol. 43, no. 28, 2010.
- [27] S. Kisseleff, W. Gerstacker, R. Schober, Z. Sun, and I. F. Akyildiz, "Channel capacity of magnetic induction based wireless underground sensor networks under practical constraints," in *Proc. 2013 IEEE WCNC*.
- [28] Z. Sun and I. F. Akyildiz, "Deployment algorithms for wireless underground sensor networks using magnetic induction," in *Proc. 2010 IEEE Globecom*.
- [29] M. Dionigi and M. Mongiardo, "Multi band resonators for wireless power transfer and near field magnetic communications," in *Proc. 2012 IEEE MTT-S*, pp. 61–64.
- [30] M. Dionigi and M. Mongiardo, "A novel resonator for simultaneous wireless power transfer and near field magnetic communications," in *Proc. 2012 IEEE MTT-S*.
- [31] C. E. Shannon, *The Mathematical Theory of Communication* University of Illinois Press, 1949.
- [32] H. Lu, J. Zhu, and S. Y. R. Hui, "Experimental determination of stray capacitances in high frequency transformers," *IEEE Trans. Power Electron.*, vol. 18, no.5 pp. 1105–1112, 2003.
- [33] A. Massarini and M. K. Kazimierczuk, "Self-capacitance of inductors," *IEEE Trans. Power Electron.*, vol. 12, no. 4 pp. 671–676, 1997.
- [34] L. Li, M. C. Vuran, and I. F. Akyildiz, "Characteristics of underground channel for wireless underground sensor networks," in *Proc. 2007 Med-Hoc-Net*.
- [35] J. R. Wait, "Criteria for locating an oscillating magnetic dipole buried in the earth," *Proc. IEEE*, vol. 59, no. 6 pp. 1033–1035, 1971.
- [36] D. R. Frankl, *Electromagnetic Theory*. Prentice-Hall, 1986.
- [37] P. Billingsley, *Probability and Measure*, 3rd ed. John Wiley & Sons, 1995.
- [38] S. Boyd and L. Vandenberghe, *Convex Optimization* Cambridge University Press, 2004.



Zhi Sun (M'11) received the B.S. degree in Telecommunication Engineering from Beijing University of Posts and Telecommunications (BUPT), and the M.S. degree in Electronic Engineering from Tsinghua University, Beijing, China, in 2004 and 2007, respectively. He received the Ph.D. degree in Electrical and Computer Engineering from Georgia Institute of Technology, Atlanta, GA, in 2011. Currently, he is Assistant Professor in the Electrical Engineering Department at State University of New York at Buffalo, Buffalo, NY. Prior to that, he was a

Postdoctoral Fellow at Georgia Institute of Technology, Atlanta, GA. Dr. Sun has won the Best Paper Award in the 2010 IEEE Global Communications Conference (Globecom). He received the BWN researcher of the year award at Georgia Institute of Technology in 2009. He was also given the outstanding graduate award at Tsinghua University in 2007. His expertise and research interests lie in wireless communications, wireless sensor networks, and cyber physical systems in challenged environments. He is a member of the IEEE.



Ian F. Akyildiz (M'86-SM'89-F'96) received the B.S., M.S., and Ph.D. degrees in Computer Engineering from the University of Erlangen-Nürnberg, Germany, in 1978, 1981 and 1984, respectively. Currently, he is the Ken Byers Chair Professor with the School of Electrical and Computer Engineering, Georgia Institute of Technology, Atlanta, the Director of the Broadband Wireless Networking Laboratory and the Chair of the Telecommunications Group at Georgia Tech. In June 2008, Dr. Akyildiz became an honorary professor with the School of Electrical Engineering at Universitat Politècnica de Catalunya (UPC) in Barcelona, Spain. He is also the Director of the newly founded N3Cat (NaNoNetworking Center in Catalunya). He is also an Honorary Professor with University of Pretoria, South Africa, since March 2009. He is the Editor-in-Chief of *Computer Networks* (Elsevier) Journal, and the founding Editor-in-Chief of the *Ad Hoc Networks* (Elsevier) Journal, the *Physical Communication* (Elsevier) Journal and the *Nano Communication Networks* (Elsevier) Journal. Dr. Akyildiz serves on the advisory boards of several research centers, journals, conferences and publication companies. He is an IEEE FELLOW (1996) and an ACM FELLOW (1997). He received numerous awards from IEEE and ACM. His research interests are in wireless sensor networks, cognitive radio networks, and nanonetworks.



Steven Kisseleff received his Dipl.-Ing. degree in Information Technology with focus on Communication Engineering from Technical University of Kaiserslautern, Germany in 2011. Currently, he is a PhD student at Institute for Digital Communications (IDC) at Friedrich-Alexander University of Erlangen-Nuremberg, Germany. His research interests lie in wireless communications, magnetic induction based signal transmissions, and wireless sensor networks in challenged environments. He is a student member of the IEEE.



Wolfgang Gerstacker (M'98-SM'12) received the Dipl.-Ing. degree in electrical engineering from the University of Erlangen-Nuremberg, Erlangen, Germany, in 1991, the Dr.-Ing. degree in 1998, and the Habilitation degree in 2004 from the same university. Since 2002, he has been with the Chair of Mobile Communications (now renamed to Institute for Digital Communications) of the University of Erlangen-Nuremberg, currently as a Professor. His current research interests include digital transmission, wireless communications and statistical signal

processing. For work on single antenna interference cancellation for GSM, he was a recipient of the IEEE COM Innovation Award 2003 and of the Vodafone Innovation Award 2004. In 2006, he received a best paper award for a publication in EURASIP Signal Processing. In 2011, he received the "Mobile Satellite & Positioning" track paper award of VTC2011-Spring. He is a Member of the Editorial Boards of IEEE TRANSACTIONS ON WIRELESS COMMUNICATIONS and *Elsevier Physical Communication* (PHYCOM), serves as a Lead Guest Editor of the Special Issue on "Broadband Single-Carrier Transmission Techniques" in 2013, and is a Co-Chair of the Cooperative Communications, Distributed MIMO and Relaying Track of VTC2013-Fall. He has served as a Member of the Editorial Board of *EURASIP Journal on Wireless Communications and Networking* (JWCN) from 2004 to 2012.